Integrated electroabsorption-modulated DFB laser by using an improved butt-joint method

Baoxia Li (李宝霞), Xiaohua Hu (胡小华), Hongliang Zhu (朱洪亮), Baojun Wang (王宝军), Lingjuan Zhao (赵玲娟), and Wei Wang (王 圩)

National Center of Optoelectronics Technology, Institute of Semiconductors, Chinese Academy of Sciences, Beijing 100083

Received November 28, 2003

An improved butt coupling method is used to fabricate an electroabsorption modulator (EAM) monolithically integrated with a distributed feedback (DFB) laser. The obtained electroabsorption-modulated laser (EML) chip with the traditional shallow ridge exhibits very low threshold current of 12 mA, output power of more than 8 mW, and static extinction ratio of −7 dB at the applied bias voltage from 0.5 to −2.0 V.

OCIS codes: 250.3140, 140.3490, 250.7360, 230.5590.

The electroabsorption-modulated laser (EML) is the most attractive and practical device for high bit rate and long haul optical communication system due to its low chirp, narrow modulated spectral linewidth, and high coupling efficiency between the electroabsorption modulator (EAM) and laser. It can contribute to reducing the system size and cost as a whole. Various integration schemes have been devised, such as selective area growth (SAG)[1], butt-coupling[2], quantum well intermixing (QWI)[3], identical active layer (IAL)[4], double stack active layer (DSAL)[5], and twin-guide structure (TGS)[6] etc.. Among them, the butt-joint integration technique is the most promising one since this approach allows independent optimization of the laser and the modulator sections.

One major difficulty in fabricating photonic integrated devices has been to reproduce good optical waveguide coupling between the functional elements. The laser and modulator share different multiple-quantum-well (MQW) structure. In conventional butt-joint integration method, different sections are grown separately using exacting selective etching followed by overgrowths. Therefore, the equipments and fabrication demands of this method are overcritical. Nevertheless, it is still difficult to create a smooth and high-quality crystal and joint geometry in the interface, and to realize high light coupling between the two waveguides.

In this paper, we demonstrate an easy way to achieve efficient butt-joint optical coupling between laser and modulator based on our existing lab condition. By using this technique, the EAM integrated distributed feedback (DFB) laser diode (LD) exhibits efficient optical coupling together with high device performance.

The structure of the device is shown in Fig. 1. First, the lower seperate confinemeat heterostructure (SCH) layer and active layers of laser were grown by low-pressure metal-organic chemical vapour deposition (LP-MOCVD) on a planar n-InP substrate. The active layers of laser are made of 5 compressive-strained InGaAsP quantum wells. After the active layers on the modulation region were partially etched off, the active layers of modulator, consisting of 9 tensile-strained InGaAsP quantum wells, were selectively grown over it. Then an upper SCH layer was grown over the entire surface. In this case, two SCH layers are perfectly continuous so as to realize efficient optical coupling between the two devices. A first-order grating was then formed on the laser region by conventional holographic lithography, which was followed by the successively growth of p-type InP cladding layer and InGaAs contact layer in the forth overgrowth process.

Micro-area photoluminescence (PL) spectra measurements at the room temperature were used to inspect the active-layer crystal quality of laser and modulator section after the first and the third growth processes,

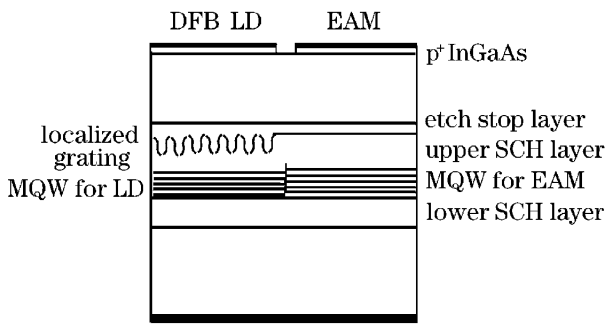

Fig. 1. Schematic diagram of integrated DFB laser and modulator with two different MQWs.

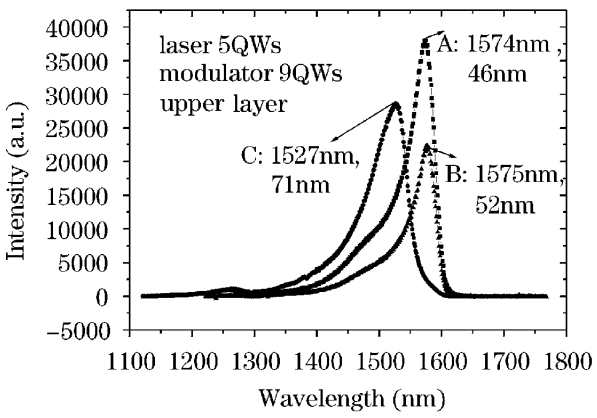

Fig. 2. PL spectra at different process stages.

respectively. The results are illustrated in Fig. 2. The line labelled with 'A' is the PL spectrum after the first growth, from which we can see the PL spectrum of laser active layers is sharp and the peak wavelength is 1.574 μm. The 'B' and 'C' lines are got after the overgrowth of the upper SCH layer, which correspond to the PL spectra of the laser section and the modulator section, respectively. Comparing the intensity and full width at half maximum (FWHM) of lines 'A' and 'B', we see the overgrowths have a certain effect on LD MQW. However, from later device performance, we can confirm this effect is slight and neglectable.

A simple ridge waveguide structure with the stripe width of 3 μm was realized in both the DFB laser and EAM section by using standard technology. The lengths of the laser and modulator are set to be 250 and 200 μm, respectively. Electrical isolation was performed by etching 50-μm-long trench through the InGaAs contact layer, followed by He^+ implantation of p-InP layer. We controlled the resistance above 50 kΩ, which provided ample margin for electrical isolation[7]. A high reflectivity coating was deposited on the rear facet to increase the output power on the front facet whereas an antireflection coating was deposited so as to reduce optical reflections back into the laser section.

The obtained EML exhibits nice single-mode operation behavior. Figure 3 demonstrates that room temperature continuous wave (CW) single-mode operation is at least maintained up to 100-mA laser driving current (output power 8 mW). The side-mode suppression ratio (SMSR) is 32 dB at injection current of 100 mA, which is great enough to be used in the wavelength division multiplexing (WDM) system.

Figure 4 shows the *P-I* characteristics of EML at different modulator bias. For zero bias, the threshold current $I_{\rm th}$ is as low as 12 mA and the optical output of EML is about 8 mW at driving current of 100 mA on the DFB laser section. All this results directly benefit from independent optimization of laser structure. As we know, the performance of threshold current and output power is better than the results reported by others[4,5,8,9]. That means our butt-joint technique can really get efficient optical coupling between laser and modulator.

Attenuation characteristics versus bias voltage shown in Fig. 5 demonstrate the static extinction ratio of near 7 dB.

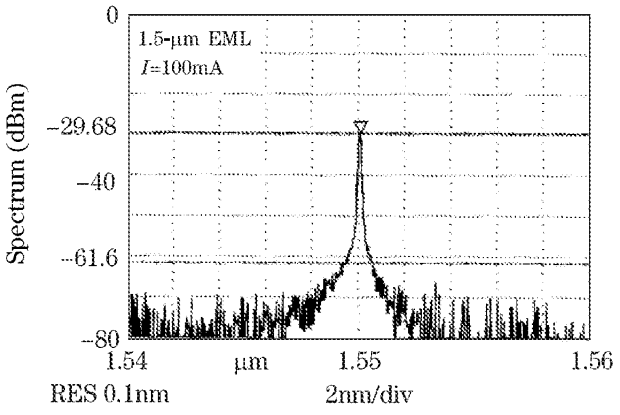

Fig. 3. The lasing spectra of EML devices.

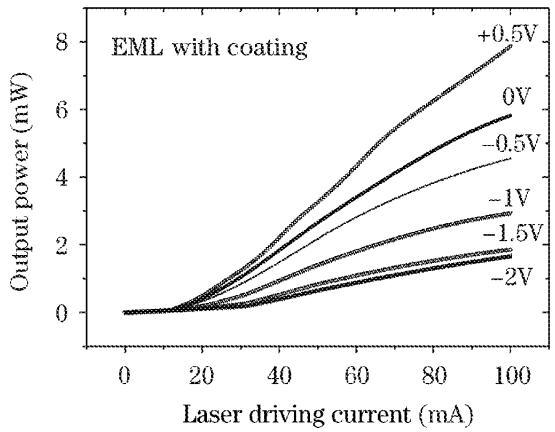

Fig. 4. The *P-I* characteristics curve at the different bias voltages applied to modulator.

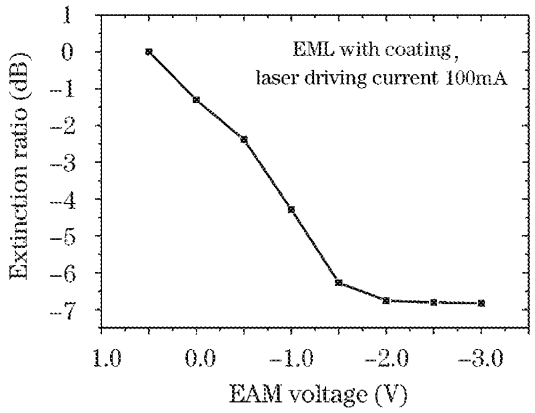

Fig. 5. EML attenuation characteristics versus applied modulator voltage.

As shown in Fig. 3, the lasing wavelength is 1.550 μm and the PL peak wavelength of the modulator active layer was measured to be 1.527 μm (Fig. 2). Thus, the detuning between them is 27 nm, which is considered far smaller than the optimization detuning setting and lead to strong optical absorption in modulator section under "on" situation of EML. Extensive work has been undertaken to optimize the detuning to further increase the output power and attenuation.

The 0.6-pF capacitance has been measured for the modulator and other dynamic parameters have been thoroughly investigated.

Monolithic integration of 1.55-μm ridge waveguide (RWG) DFB LD with EAM using an improved butt-joint method is demonstrated. This device exhibits very promising static performance, including 12-mA threshold current, 8-mW output optical power. All these attractive results greatly benefit from independent optimization of laser and modulator structure, which is only possible by using butt-joint integration scheme.

This work was supported by the National "973" Project of China (No. G20000683-1), the National "863" Project of China (No. 2001AA312050), and the National Natural Science Foundation of China (No. 90101023). B. Li's e-mail address is lbxia@red.semi.ac.cn.

References

1. M. Aoki, M. Suzuki, H. Sano, T. Kawano, T. Ido, T. Taniwatari, K. Uomi, and A. Takai, IEEE J. Quantum Electron. **29,** 2088 (1993).
2. H. Takeuchi, K. Tsuzuki, K. Sato, M. Yamamoto, Y. Itaya, A. Sano, M. Yoneyama, and T. Otsuji, IEEE J. Sel. Top. Quantum Electron. **3,** 336 (1997).
3. R. L. Thornton, W. J. Mosby, and T. L. Paoli, J. Lightwave Technol. **6,** 786 (1988).
4. M. Le Pallec, C. Kazmierski, E. Vergnol, S. Perrin, J. G. Provost, P. Doussière, G. Glastre, D. Carpentier, and S. Fabre, IEEE Photon. Technol. Lett. **15,** 362 (2003).
5. B. Stegmueller, E. Baur, and M. Kicherer, IEEE Photon. Technol. Lett. **14,** 1647 (2002).
6. O. Sahlén, L. Lundqvist, and S. Funke, Electron. Lett. **32,** 120 (1996).
7. R. A. Salvatore, R. T. Sahara, M. A. Bock, and I. Libenzon, IEEE J. Quantum Electron. **38,** 464 (2002).
8. B. Stegmueller, R. Gessner, F. Kunkel, J. Rieger, M. Schier, J. Walter, and E. Baur, in *Optoelectronic and Microelectronic Materials and Devices Conference Proceedings* 9 (2000).
9. H. Kawanishi, Y. Yamauchi, N. Mineo, Y. Shibuya, H. Murai, K. Yamada, and H. Wada, IEEE Photon. Technol. Lett. **13,** 954 (2001).